J Musculoskelet Neuronal Interact 2022; 22(2):203-211

Journal of Musculoskeletal and Neuronal Interactions JMNI

Original Article

Validation of High-Resolution peripheral Quantitative Computed Tomography-Derived Achilles Tendon Properties Against Diagnostic Ultrasound

Hugo J.W. Fung[1,2], Angela M. Cheung[2,3,4,8], Sunita Mathur[5,6], Eva Szabo[2,8], Andy K.O. Wong[2,4,6,7,8]

[1]Department of Exercise Science, Faculty of Kinesiology and Physical Education, University of Toronto, Canada;
[2]Centre of Excellence in Skeletal Health Assessment, University of Toronto, Toronto, ON, Canada;
[3]Department of Medicine, University Health Network, Canada;
[4]Toronto General Hospital Research Institute, University Health Network, Toronto, ON, Canada;
[5]Department of Physical Therapy, Faculty of Medicine, University of Toronto, Canada;
[6]Rehabilitation Sciences Institute, Faculty of Medicine, University of Toronto, Canada;
[7]Department of Epidemiology, Dalla Lana School of Public Health, University of Toronto, Canada;
[8]Osteoporosis Program, Schroeder's Arthritis Institute, University Health Network

Abstract

Objectives: 1) To assess the precision of high resolution peripheral quantitative computed tomography (HR-pQCT)-derived Achilles tendon (AT) cross-sectional area (HR AT-CSA) and density, and 2) to validate HR AT-CSA against ultrasound-derived AT-CSA (US AT-CSA). **Methods**: Women and men (≥50 years) had HR-pQCT (0.082mm isotropic) and US scans (B-mode) performed on the non-dominant ankle. Linear regression and Bland-Altman analyses assessed systematic differences between HR-pQCT and US-derived AT-CSA. Precision measured by % root mean square coefficients of variation (%RMSCV) and agreement by type 2,1 intraclass correlation coefficients ($ICC_{2,1}$), were determined for test-retest US AT-CSA scans, and analysis-reanalysis of 30 HR-pQCT and US images. **Results**: Among 44 participants, HR and US AT-CSA were strongly correlated (R^2=0.84, p<0.01, B=1.05[0.90–1.19]), with no differences between modalities (p=0.37). Bland-Altman analysis revealed minimal systematic bias (-0.7mm^2[-10.7–9.3]; 1.3%) between HR-pQCT and US-derived AT-CSA with smaller AT-CSA values showing larger inter-modality differences (R^2=0.098, B=-0.137 [-0.268–-0.008], p=0.039). US AT-CSA demonstrated excellent test-retest precision ($ICC_{2,1}$=0.998, %RMSCV=1.04%). Analysis-reanalysis of HR-pQCT AT-density and both HR-pQCT and US AT-CSA displayed $ICC_{2,1}$ above 0.95 and %RMSCV within 3%. **Conclusion**: HR-pQCT can examine AT-morphometry with acceptable analytical precision. Future studies should explore these metrics' association with functional outcomes and ankle-bone structural and mechanical properties.

Keywords: Achilles Tendon, HR-pQCT, Tendon Cross-Sectional Area, Tendon Density, Ultrasound

Introduction

High-resolution peripheral quantitative computed tomography (HR-pQCT) is a well-validated tool for quantifying bone volumetric density and microarchitecture at distal appendicular sites such as the radius and tibia[1]. Further, evaluations of HR-pQCT scans using finite element analysis can determine failure load, load distribution across cortical versus trabecular bone, and Young's modulus[2,3]. Previously, Erlandson et al., successfully quantified myotendinous tissue cross-sectional area and density, segmented from distal tibia HR-pQCT scans, using a custom threshold-based algorithm[4]. Within these segmentations, the Achilles tendon (AT) constitutes a proportion of the myotendinous tissue. To our knowledge, no studies have looked at the specific use

Andy K.O Wong was funded by a Toronto General Hospital Research Institute Fellowship Award at the time of completion of this study and is currently funded by an Arthritis Society Career Salary Award. Angela M. Cheung was funded by a Tier 1 Canada Research Chair award in Musculoskeletal and Postmenopausal Health. The remaining authors have nothing to declare.

Corresponding author: Andy Kin On Wong, 200 Elizabeth St. Toronto General Hospital Research Institute , 7EN-238, Toronto, ON M5G 2C4, Canada
E-mail: andy.wong@uhnresearch.ca

Edited by: G. Lyritis
Accepted 12 January 2022

of HR-pQCT for quantifying tendon properties *in vivo*. With the recent interest in studying the impact of muscle on bone health[5,6], and given tendon's role in transducing forces from muscle to bone, it is critical to further understand the extent that tendon contributes to the influence of muscle on bone. As such, it is important to identify modalities that would allow for the collection of bone, muscle, and tendon parameters within an individual.

Currently, tendon morphology is primarily assessed with either magnetic resonance (MR) or ultrasound (US) imaging, both of which have their respective advantages and limitations for tendon imaging. US imaging is often chosen over MRI due to its ease of use, access, low cost, and versatility[7,8]; however, a major disadvantage for US is that it is one of the most operator-dependent imaging modalities, whereby the value of the diagnostic information generated depends largely on the operators' expertise[8]. When examining AT morphology, specifically AT cross-sectional area (AT-CSA), Kruse et al., suggested that while both MRI and US measures of proximal and distal AT-CSA show good reliability separately (US $ICC_{(2,2)}$: 0.84-0.89; MRI $ICC_{(2,2)}$: 0.94-0.97), they should not be used interchangeably as US delivered systematically smaller AT-CSA values (~5.5% or ~3.2 mm^2, $p<0.001$) when compared to MRI[9].

Although both US and MRI are primarily used to assess soft-tissues, recent advancements in US assessments have allowed for the surrogate measurement of bone mineral density (BMD)[10,11], whereas MRI has also yielded estimates of bone microarchitecture[12-14]. However, BMD estimation by quantitative US is limited by scan location, as most available sonometers can only assess the calcaneus[15]; further, this US-derived surrogate for BMD is less accurate when compared to values generated by ionizing imaging modalities (i.e., Dual-energy X-ray Absorptiometry (DXA) or QCT)[10]. In addition, MRI is not directly suited for assessing BMD, as MRI is based on differences in proton relaxation properties, hence there is no calibration to physical densities[14]. As such, the possibility of extending HR-pQCT's ability, from quantifying BMD and bone microarchitecture, to further obtain measures of tendon CSA and density may potentially reduce costs by avoiding the need for additional imaging and enhancing research output.

Traditionally, tendon density is measured through *ex vivo* physical mass-density (g/cm^3), which is often approximated by comparison to the density of a similar tendon (patellar tendon), as 1.6 g/cm^3 [16]. Larger tendon mass density has been associated with better mechanical properties (e.g., ultimate tensile strength, elastic modulus, and strain energy density)[16]. Human AT total mass consists of approximately 70% water, while collagen accounts for about 80% of the dry mass[17]. With overuse, injury, and pathologies, the AT structure and extracellular matrix composition is altered, including elevated expressions of type I and III collagen[18,19], alterations in fibrillar alignment, an increase in larger hydrophilic proteoglycans resulting in an increase in bound water and tendon thickening[20,21], a high density of inflammatory cells (for overuse and injury, but debatable for pathologies – dependent on the chronicity of the condition)[22], and potentially infiltration of fat[23]. Since CT scans can determine Hounsfield units, a measure of tissue density relative to water, it is possible that these tendon compositional changes can be reflected by the linear attenuation coefficient (i.e., radiodensity).

Schepull & Aspenberg were the first to use radiodensity, as measured by conventional CT, to evaluate the healing of ruptured AT[24]. They determined that about 80% of the variability in AT elastic modulus was explained by radiodensity. However, the reproducibility and biases of their radiodensity acquisition methods were not evaluated. HR-pQCT, which is a higher resolution CT modality (voxel size ~82 um isotropic versus 512 um in-plane) has significantly lower radiation, is specialized for imaging appendicular sites, and has been used previously to examine myotendinous tissues[4]. As such, there is a need to address whether HR-pQCT can feasibly and reliably quantify tendon radiodensity, henceforth referred to as HR-pQCT-derived AT density.

Our study aimed to assess the analysis-reanalysis precision of HR-pQCT-derived AT-CSA and density using the custom soft tissue analysis algorithm from the HR-pQCT manufacturer[4], and to validate the HR-pQCT-derived (HR) AT-CSA against ultrasound-derived (US) AT-CSA as a reference standard. We hypothesize that: (1) HR AT-CSA and density have high analysis-reanalysis reproducibility (Percentage root-mean square coefficient of variation (%RMSCV) <5%), (2) a moderate correlation ($r>0.6$) exists between HR and US AT-CSA, and (3) the difference between AT-CSA obtained by US versus by HR-pQCT will not be statistically significant ($p>0.05$).

Materials and Methods

Subjects

The current study is a cross-sectional analysis of a larger observational study measuring bone and muscle quality in older adults using imaging and functional testing[25]. As part of the original study aim, participants underwent medical imaging (HR-pQCT, DXA, and US) procedures to investigate how bone, muscle, and tendon characteristics relate to the risk of falls and fractures. This report represents an ancillary component of the study. Physical activity and medical history questionnaires, isometric ankle strength, and balance test outcomes were also collected but not included in this analysis. A convenience sample of participants were recruited by poster advertisement located throughout local academic hospitals and by word of mouth. Both women and men were included if age was ≥50 years and excluded if they had a history of ankle fractures, metal implants in either legs, or had muscle and/or AT disorders (i.e., self-reported Achilles tendonitis or tendinopathies).

The present analysis only includes participants who have completed both HR-pQCT and US scans. The examined leg was on the contralateral side to the dominant writing hand. Participants gave informed consent prior to any study procedures. The protocol for this study was approved by the University Health Network (14-8163-AE) and University of Toronto (31266) Research Ethics Boards and conformed to the standards set by the *Declaration of Helsinki*.

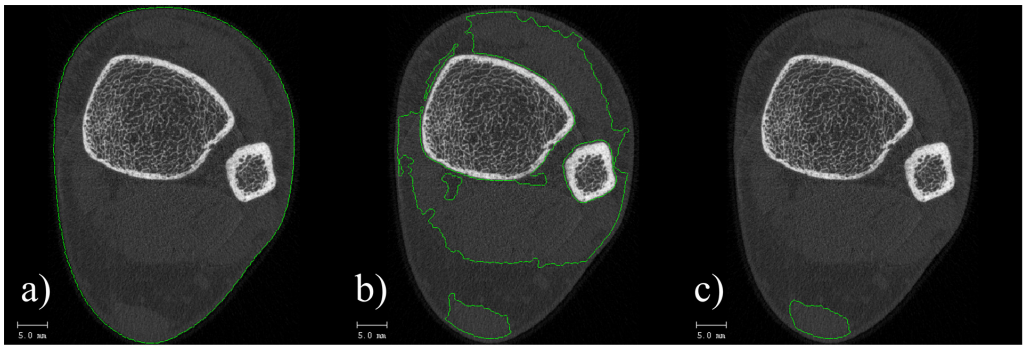

Figure 1. Illustration of progression from limb contour, to application of custom thresholds (34.22 – 194.32 mg HA/cm^3) a) Semi-automatic generation of limb contours using threshold algorithm b) Muscle and myotendinous tissue contours generated by Soft-Tissue Analysis script c) Resulting Achilles tendon contour following removal of muscle and myotendinous tissue contours with manual refinement (when necessary). These cleaned Achilles tendon contours subsequently underwent tendon analysis. HA, hydroxyapatite.

Measurement of Achilles Tendon Cross-Sectional Area

HR-pQCT

Participants underwent HR-pQCT (XtremeCT, Scanco Medical AG, Basserdorf, Switzerland) scans of the distal tibia at the University of Toronto Centre of Excellence in Skeletal Health Assessment - Toronto General Hospital site. Scans were obtained following standard imaging protocols (110 trans-axial CT slices in the proximal direction with isotropic voxel resolution of 82 µm^3 at 22.5 mm proximal to the tibial endplate with the following settings: 60 kVp X-ray tube current of 95 mA, matrix size 1535 x 1536)[3]. These scans captured both the AT and the distal tibia bone microarchitecture. The effective dose of radiation imposed by this scan was 3 µSv per measurement (i.e., less than half of the background radiation received on an average day (8 µSv). As required by the regulations in Ontario, Canada, a medical radiation technologist performed the scans. Positioning for the scans were done by a single trained operator (ES). Hydroxyapatite phantoms were scanned daily for quality control.

Ultrasound

The diagnostic ability of US is operator-dependent; as such, a single operator (HJWF) was trained by a sonographer, on a cohort of mixed-sex healthy young adults (test-retest RMSCV <5%), to perform all US imaging at the University of Toronto – Muscle Function & Performance Lab, using a GE LOGIQ E Portable USI System (GE Healthcare, Waukesha, WI) with 2-dimensional, high-frequency (8-12 MHz) linear transducer using B-mode imaging and exam category "small parts" (gain: 86-94, depth: 3.5-4.0 cm, frequency: 12 MHz).

Participants were asked to lay prone on an examination plinth with socks and shoes removed, and with both heels overhanging in a naturally relaxed position to expose the AT. Sandbags were placed on either side of the lower leg to minimize movement during the scan. The examiner palpated and marked the mid-aspect of the medial malleolus, to approximate the tibial endplate. This mark was then traced onto the posterior aspect of the ankle, where a line 22.5 mm proximal from this reference point was manually measured and marked to signify the acquisition location. This acquisition site approximated the HR-pQCT scan region of interest as described above.

Using a protocol adapted from Pang et al, a transverse scan of the marked acquisition location produced a trans-axial image of the AT[26]. Images were examined to ensure that the boundaries of the AT were visually discernable. These images, from which AT-CSA values were derived, were repeated in triplicate and were used for assessing test-retest reproducibility.

Image Processing & Analysis

HR-pQCT

Prior to processing and analyses, all HR-pQCT images were graded for motion and must not have exceeded a grading of 3, in accordance with expert guidelines to obtain acceptable measurement quality[27]. For the AT analysis, an updated version (Ver. 1.1, SCANCO Medical AG, Bruettisellen, Switzerland) of the Soft-Tissue Analysis algorithm reported by Erlandson et al., was used to segment muscle and myotendinous tissues[4]. The main updates in Ver 1.1 included implementation of 3-dimensional speckle/island removal at an earlier stage (compared to previous 2-dimensional removal, occurring later in the script), and a revamped definition of the subcutaneous layer. We refer readers to the study by Erlandson et al. for more details regarding the custom threshold-based algorithm[4]. Briefly, a semi-automatic threshold-based algorithm was applied to the tibia scans to generate contours of the entire limb. Subsequently, the Soft-Tissue Analysis script was applied to the limb contour to identify and isolate the soft tissue components, producing contours of muscle and myotendinous tissue. From

these contours, the AT was isolated by deleting surrounding muscle segmentations. In cases where the AT was poorly segmented, manual correction was performed. An example of the resulting AT segmentation is shown in Figure 1.

30 randomly selected HR-pQCT scans were de-identified (ES) for blinded analysis-reanalysis by the same operator (HJWF) to determine analysis-reanalysis precision error. To reduce potential bias, all re-analyses were performed on a separate date from the original image analyses. Outputs generated by the analysis included tendon density (mg/cm^3) and AT volume (mm^3), each measured across the full image stack. AT-CSA (mm^2) was calculated for comparison against US by dividing the AT volume by the total stack height (110 slices x 0.082 mm/slice=9.02 mm).

Ultrasound

All sonographs were analyzed offline, in DICOM format, using a freely available image analysis software package (OsiriX Lite, Pixmeo, Geneva, Switzerland)[28]. AT-CSA was ascertained by manually outlining the visible borders of the AT, for each of the 3 CSA scans (Figure 2). US AT-CSA precision was calculated as the test-retest reliability of AT-CSA images collected in triplicates. To determine analysis-reanalysis reproducibility, blinded analysis of 30 images were performed twice on the same set of images by a single operator (HJWF). Similar to the HR-pQCT image analysis protocol, these 30 images were randomized prior to both analysis and reanalysis, where re-analyses occurred on a separate date from the original analysis to ensure minimal bias. Since US is known to be one of the most operator-dependent imaging modalities, test-retest analyses for the US AT-CSA measures were performed on one set of the replicates to ensure that the sonographer (HJWF) met the reproducibility standards previously published in the literature.

Statistical Analysis

Normality of all variables were assessed both visually (Histogram, Q-Q plot) and statistically with the Shapiro-Wilk's test. Precision error was assessed using %RMSCV for both test-retest analysis of US AT-CSA and analysis-reanalysis of both HR-pQCT and US-derived AT-CSA. Absolute agreement for these precision estimates were quantified using a type 2,1 intraclass correlation coefficient for single observers ($ICC_{2,1}$). Validity of HR-pQCT against US-derived AT-CSA was further evaluated with linear regression and systematic bias evaluated using graphical Bland-Altman analysis. Univariate linear regression was performed between difference and means to evaluate for possible trends within the Bland-Altman plot. Paired-samples t-test assessed the hypothesis that no significant difference exists between HR- and US-derived AT-CSA. All data analyses were conducted using IBM SPSS Statistics (v.20). Statistical significance was set at α=0.05.

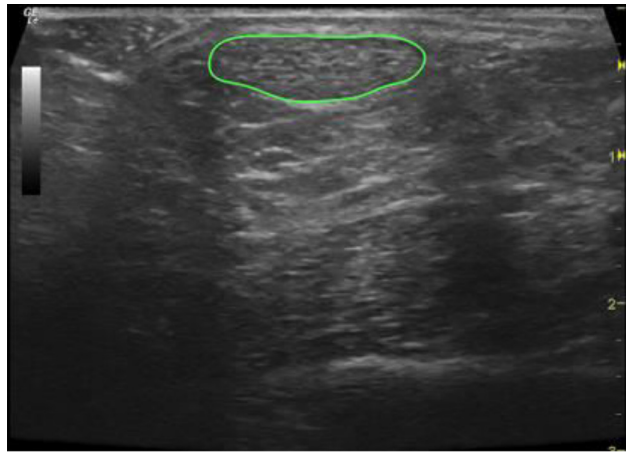

Figure 2. Trans-axial view of the Achilles tendon through Ultrasound. Contour denotes manual segmentation of the Achilles tendon using OsiriX.

Results

Participant Characteristics and AT Measurements

Of the 111 participants successfully recruited into the overarching study, 13 did not complete the study protocol due to personal reasons. Of the remaining 98 enrolled in our study, 97 had completed HR-pQCT scans of the distal tibia; of those participants, 45 completed US scans of their AT. Only one participant's HR-pQCT distal tibia scan exhibited motion grade ≥3 and was therefore excluded from analyses to ensure that the precision of parameters were not influenced by image quality. Analyses were performed in 44 participants who completed both HR-pQCT and US imaging of the AT.

The demographics of the 44 participants and their respective AT morphometry, separated by sex, are detailed in Table 1. Participants were predominantly (75%) female, with mean BMI in the overweight category for both sexes (Table 1). Scans were performed on the non-dominant side, majority being on the left leg (93%). Significant between-group differences were observed between males and females, with respect to their height, weight, and both HR- and US- derived AT-CSA. Compared to the female participants, the males in our study were taller, heavier, and had larger AT-CSA values across both imaging modalities.

As part of the overarching study, we collected information regarding steroid use, physical activity levels using the physical activity scale for the elderly (PASE), and degenerative/metabolic/inflammatory diseases of the participants. From our 44 participants, 11 individuals had previously taken corticosteroids regularly or daily, 7 were diagnosed with osteoporosis, 10 were diagnosed with osteoarthritis, 2 with rheumatoid arthritis, and one individual had type-2 diabetes. Additionally, 8 individuals were regular

Table 1. Participant characteristics comparison between men and women.

Variable	Men (n=11)	Women (n=33)	Pooled (n=44)	p-value
Age (years)	63.7 ± 10.0	61.5 ± 8.5	62.1 ± 8.8	0.487
Height (m)	1.73 ± 0.04	1.61 ± 0.09	1.64 ± 0.09	**< 0.001**
Weight (kg)	81.1 ± 13.2	66.8 ± 17.6	70.6 ± 17.1	**0.018**
BMI (kg/m^2)	27.1 ± 3.9	25.7 ± 6.4	25.9 ± 5.5	0.508
HR AT Density (mg/cm^3)	20.8 ± 1.08	20.0 ± 2.39	20.2 ± 2.16	0.280
HR AT-CSA (mm^2)	63.6 ± 7.4	51.0 ± 10.4	54.1 ± 11.1	**< 0.001**
US AT-CSA (mm^2)	66.2 ± 7.8	51.1 ± 11.7	54.8 ± 12.7	**< 0.001**

All values are presented as Mean ± Standard Deviation. Bolded p-Value indicates significant difference (p<0.05) between sexes, determined by univariate analysis of variance (ANOVA). Abbr: BMI, body mass index; HR AT-CSA, high-resolution peripheral quantitative computed tomography; US, ultrasound; AT-CSA, Achilles tendon cross-sectional area.

Table 2. Measures of Analysis-Reanalysis Precision - $ICC_{2,1}$ Single Measures [95% CI], %RMSCV.

	AT Cross-Sectional Area		AT Density
	HR-pQCT	US	HR-pQCT
$ICC_{(2,1)}$ Single Measures	0.959 [0.916 – 0.980]	0.998 [0.996 – 0.999]	0.965 [0.928 – 0.983]
%RMSCV	2.83%	1.04%	1.97%

Calculations were based on blinded analysis-reanalysis of 30 randomly selected HR-pQCT, as well as 30 randomly selected US scans. ICC, intraclass correlation coefficient; %RMSCV, % root mean squared coefficient of variation; HR-pQCT, high-resolution peripheral quantitative computed tomography; US, ultrasound; AT, Achilles tendon.

smokers in the past. Collectively, our study participants had a PASE score of 213.4±110.7, with males being more physically active than female participants (313.5±105.8 and 189.3±99.5, respectively; p=0.011).

AT Parameters

The three US AT-CSA measures per participant demonstrated excellent test-retest precision, as evidenced by an $ICC_{2,1}$ of 0.971, 95% CI [0.953 – 0.983], and %RMSCV of 3.68%. Analysis-reanalysis precision of both HR-pQCT and US AT-CSA, as well as HR-pQCT acquired tendon density, were all acceptable, with $ICC_{2,1}$ single measure values being above 0.95, and %RMSCV being within 3%. Analysis-reanalysis precision of US-derived AT-CSA was slightly better than that of HR-AT-CSA measurements (Table 2).

HR-pQCT and US-derived AT-CSA were strongly correlated, with 83.9% of the variability seen in US AT-CSA explained by the variation in HR AT-CSA (R^2=0.839, p<0.001) and a validation regression coefficient near unity (B=1.05 with 95% CI [0.90 – 1.19]) with systematic error (intercept) of -1.78 mm^2 (Figure 3). Mean HR AT-CSA was smaller than mean US AT-CSA (M±SD; 54.1±11.1 mm^2 and 54.8±12.6 mm^2, respectively); however, paired-samples t-test determined this difference was not statistically significant, t(43)=-0.91, p=0.37, 95% CI of difference scores [-2.3 mm^2 – 0.8 mm^2]. Agreement between HR-pQCT and US-derived AT-CSA was assessed by the Bland-Altman method (Figure 4). On average, the HR-pQCT estimate was 0.7 mm^2 smaller compared to the reference standard US-derived estimate, resulting in a negative bias of 1.27%. Despite no apparent trend in our Bland-Altman plot from visual inspection, regression analyses between the average AT-CSA and the difference between HR and US AT-CSA determined a slight negative systematic bias, showing the magnitude of difference was larger for the more extreme ends of AT-CSA values (R^2=0.098, B=-0.137[-0.268 – -0.008], p=0.039) (Figure 4).

Discussion

This cross-sectional study used HR-pQCT images to quantify structural properties of the AT, specifically CSA and density. We found that HR-derived AT parameters can be analyzed with high precision (<5% error) and is well-validated when compared against the reference standard of US. Test-retest reproducibility of US-derived AT-CSA met ISCD standards of being within 5% error and is consistent with benchmarks previously published[9,29,30]. While the HR AT-CSA values were slightly smaller (0.7 mm^2) compared to that of US AT-CSA, this difference was not statistically significant (p=0.37). Further, we observed a robust correlation in AT-CSA between the modalities

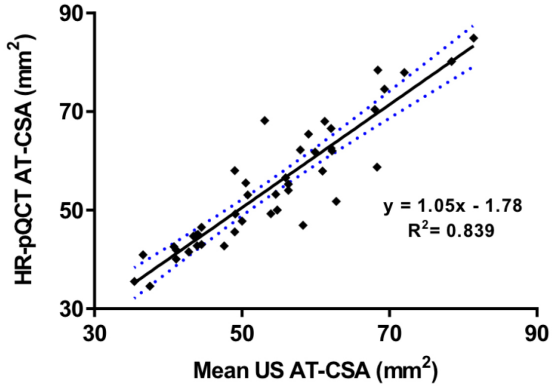

Figure 3. Linear regression between HR-pQCT and Ultrasound-derived Achilles tendon cross-sectional area. Regression Coefficient=0.916 (p<0.01), B[95% Confidence Interval]= 1.05[0.91-1.19]; HR-pQCT, High-resolution peripheral quantitative computed tomography; US, ultrasound; AT-CSA, Achilles tendon cross-sectional area.

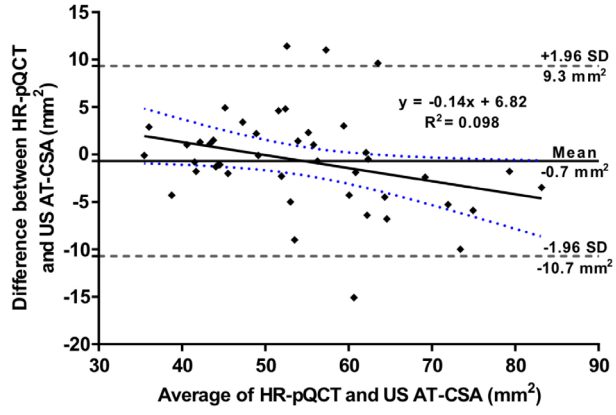

Figure 4. Bland-Altman Plot Between HR-pQCT and US AT-CSA for Analysis of Agreement. Bland-Altman Plot displays the mean difference, 95% limits of agreement. Mean difference (bias)±SD between HR-pQCT and US AT-CSA was -0.7±5.1 mm². Simple regression analyses denote a slight but significant negative trend (R^2=0.098, B=-0.137[-0.268 - -0.008], p=0.039). HR-pQCT, High-resolution peripheral quantitative computed tomography; US, ultrasound; AT-CSA, Achilles tendon cross-sectional area.

(R^2=0.839, B=1.05[0.90 – 1.19], p<0.001), demonstrating the validity of using HR-pQCT to measure AT-CSA.

Our results demonstrate the feasibility of the Soft Tissue Analysis algorithm, by Scanco, for quantifying AT-CSA and density from existing HR-pQCT images, which are traditionally used for measuring bone strength and micro-architecture. The potential to utilize one scan to quantify tendon properties, beyond the already reported bone parameters, ultimately reduces the need to order additional medical imaging and will help to further the understandings of the muscle-tendon-bone axis on musculoskeletal health. It is well known that the loading of bones, specifically through exercise, can provide an anabolic stimulus to maintain bone health[31]. Despite the growing literature on the influence of muscle for maintaining bone health, the relationship between tendons and bone health remains poorly studied. Since muscles require tendons to transduce forces onto bone, there is a need to further investigate how specific properties of tendons can affect the quality of bone, for example its architecture, density, and porosity. Although not examined in the present study, HR-pQCT scans can also be analyzed with finite element analysis[32], which can further provide insight into the mechanical properties (e.g., axial failure load, stiffness, stress, etc.) of the tendon. While these values have yet to be tested and correlated to *ex vivo* tendon failure loads, the potential to determine tendon mechanical properties in-vivo would be monumental. Distal tibia scans have previously been obtained using HR-pQCT to measure *in vivo* bone microstructure – those with access to datasets of HR-pQCT distal tibia scans can now perform retrospective analyses to generate tendon measures, allowing for the possibility to look at inter-individual differences, changes in tendon density and CSA over time, and ultimately open the door to a wealth of bone-tendon interaction studies.

Contrary to the previous version (Ver 1.0) of the Soft Tissue Algorithm utilized by Erlandson et al., the new soft-tissue analysis can generate contours that more tightly fit the AT[4]. Compared to the older version, this update was able to perfectly segment out the AT in roughly 16% of our HR-pQCT images (7/44 individuals), circumventing the need to perform manual correction of the generated contours. Ultimately, this capacity translated to an enhanced precision and reproducibility of HR AT-CSA values; this improvement was seen through comparison to HR AT-CSA measures of the same dataset when we used soft-tissue analysis Ver 1.0 for segmentation (HR AT-CSA: 68.1±13.5 mm², %CV=9%, $ICC_{2,1}$=0.742).

The observed analysis-reanalysis precision errors for HR AT-CSA and tendon density were artificially lower than test-retest values because they were free of variability in X-ray beam properties, object interactions, and positioning error. The additional variability from repositioning during HR-pQCT test-retesting, which had been previously shown as a major contributor to scanning precision error[33], could present as differences in angulation of the tendon relative to the gantry that could translate to larger AT-CSA differences. While this may be true, densitometric measures are less sensitive to positioning-associated errors (i.e., shifts in geometry) as demonstrated by their greater reproducibility compared to architectural measurements (e.g., trabecular thickness)[34]. Despite the present study not measuring test-retest precision, which accounts for repositioning error, HR-

pQCT test-retest scans of the distal tibia measuring bone microarchitecture, muscle, and myotendinous parameters remains to have excellent precision (<2%)[4,35]. With HR AT-CSA and density showing low analytical error (2.83 vs 1.97 %RMSCV, respectively) (Table 2), we anticipate that test-retest precision for HR-pQCT derived AT-CSA and density would still remain within 5% error. However, our hypothesis needs to be validated, as future studies should look at precision error associated with AT measurements from test-retests of HR-pQCT scans.

We determined that the analysis-reanalysis precision error of HR AT-CSA was higher than US AT-CSA (2.83% vs 1.04% respectively) (Table 2). From these precision measures, it is possible to further calculate the least significant change (LSC), a quantitative metric for ensuring observed differences are larger than precision errors associated with a technique[36,37]. As such, we were able to approximate with 95% confidence that the LSC (LSC_{95}) for HR and US AT-CSA, based on 30 patients with duplicate analyses, were 7.84% and 2.87% respectively. This implies that a 7.84% difference between repeat AT-CSA analyses must be present for the HR-pQCT to determine that an actual change has occurred, rather than being attributed to imprecision. Indeed, it is important to emphasize that these LSC's were calculated from repeated analyses of scans from 30 patients; as such, the test-retest LSC's will be potentially larger due to the inclusion of positioning variability. With endurance exercise training, AT hypertrophy as measured by AT-CSA has been shown to increase between 7.2 to 8.5%[38,39]. By contrast, Romero-Morales et al., showed that individuals with Achilles tendinopathy displayed a ~51.1% greater AT-CSA, averaged between two measurement sites, compared to age, height, and weight-matched controls[40]. Accordingly, the HR-pQCT would potentially be a valid tool to assess such pathological changes in the AT. However, seeing that the analysis-reanalysis LSC_{95} for HR AT-CSA is within the observed range of exercise-induced changes, the HR-pQCT may potentially lack the necessary precision to determine AT-CSA changes with exercise training. Accordingly, future studies should determine the test-retest LSC_{95} for HR AT-CSA to examine whether the HR-pQCT has the necessary sensitivity to precisely detect AT-CSA changes. In addition, as greater AT-CSA hypertrophy has been shown with longer durations of exercise training[38], future studies should examine whether there exists a temporal threshold with training duration to exceed the HR AT-CSA test-retest LSC_{95}.

Previously, Kruse et al., saw that US-derived AT-CSA was statistically smaller (~5.5%, $p<0.001$) compared to AT-CSA obtained by MRI[9]. As a result, Kruse et al., suggested that US and MRI cannot be used interchangeably for AT-CSA assessments[9]. In contrast, our results showed a non-statistically significant difference between HR and US AT-CSA, where HR-pQCT-derived values were on average ~1.3% smaller, demonstrating comparable AT-CSA measurements between the two modalities. It is important to highlight that a linear regression analysis of our Bland-Altman plot determined a slight but statistically significant negative trend of differences, where HR AT-CSA values appear to be consistently greater than US AT-CSA values, until ~60 mm^2 where HR AT-CSA appears to be consistently smaller than US AT-CSA. However, the strength of association between paired AT-CSA differences and means is weak ($r=0.31$). Although this negative trend is visually evident, the observed correlation does not detract from the observed precision and reliability of HR-pQCT to quantify AT-CSA.

In our study, some limitations related to the US measurement could have influenced our results. Kruse et al., previously noted that probe pressure can result in up to 6% variance in AT-CSA and/or thickness[9]. In our study, we did not use any equipment to control the probe pressure beyond having the US operator attempt to maintain consistent pressure throughout examinations; however, even with this variability in probe pressure, our results met the US reproducibility standards published previously in the literature, demonstrating an amount of bias consistent with that reported before[9,29,30]. Further, the method used to approximate the HR-pQCT scan site through estimating the tibial endplate location via the medial malleolus may not be entirely accurate. The AT varies in CSA, particularly at the more distal location[41]; as such, the inability to replicate the exact HR-pQCT scan site for US may have influenced our results.

Prior to US examination of the AT, participants had completed isometric unilateral contractions of the ipsilateral ankle flexors. Slow muscle contractions (i.e., slow concentric or isometric contractions) alter the viscoelasticity of tendons by breaking collagen cross-links, ultimately decreasing tendon stiffness. Wearing et al., stressed the importance of employing tendon pre-conditioning exercises prior to sonographic determination of AT morphology, specifically thickness, as it results in increased association with other variables due to standardizing the load history of the AT and changes in the fluid content of tendon matrix[42,43]. However, in our study, HR-pQCT scans at the ankle were obtained prior to any ankle flexion exercises, and thus this differential timing may play a role in some of the discrepancies seen between HR and US AT-CSA.

In its current state, we do not suggest the use of HR-pQCT-derived AT measures for clinical diagnoses or management; however, our present study sheds light on the ability of HR-pQCT as a viable research tool for evaluating bone, muscle, and now tendon properties. Consequently, we hope these findings motivate future studies to investigate the relationship between tendon-muscle-bone quality. Future studies should investigate the role of AT-CSA and tendon density, to determine if they are related to functional outcomes, such as torque, rate of force development by muscle groups, and balance. Tendon density could potentially be a surrogate for tendon collagen cross-linking, which alters AT stiffness, affecting the ability of the AT to store and convert potential energy into mechanical force. As such, it is important to determine whether HR-pQCT-derived AT density can be considered a novel biomarker for improving clinical correlations by comparing it against validated

measures of mechanical, structural, and biochemical properties using ultrasound elastography, multi-modal MRI, or histopathological findings. In addition, finite element analysis has been applied to HR-pQCT scans to measure bone strength (i.e., failure load, stiffness, etc.)[32]. Future studies should investigate how tendon properties relate to bone microarchitecture and mechanical strength parameters, all derived within the same HR-pQCT scan.

Conclusion

In conclusion, the analysis of HR-pQCT distal tibia scans for AT-CSA and density was precise. Our results suggest that AT-CSA measured using HR-pQCT is valid and comparable to US-derived values. Distal tibia scans have been previously obtained using HR-pQCT, thus retrospective analyses of the AT can be performed on these same scans to provide a wealth of information and allow for further probing of bone-tendon interactions. Future studies should utilize the potential of HR-derived AT morphometric properties to examine their relationship with muscle functional outcomes or ankle and calcaneal bone structural and mechanical properties.

Acknowledgements

We would like to thank all participants from the Ankle Fracture Study for their involvement with the study. Andy Kin On Wong, Sunita Mathur, and Angela Cheung are wholeheartedly thanked for their continued support throughout Hugo Jern Wai Fung's undergraduate training, resulting in the completion of his undergraduate thesis, which enabled this work.

Authors' Contributions

H.J.W.F., A.M.C., S.M., and A.K.O.W. conception and design of research; H.J.W.F, E.S. and A.K.O.W. conducted the research; H.J.W.F. and A.K.O.W. analyzed the data; H.J.W.F and A.K.O.W. drafted the manuscript; H.J.W.F., A.M.C., S.M., E.S., and A.K.O.W., edited and revised the manuscript, and approved final version.

References

1 Burghardt AJ, Buie HR, Laib A, Majumdar S, Steven K. Reproducibility of Direct Quantitative Measures of Cortical Bone Microarchitecture of the Distal Radius and Tibia by HR-pQCT. Bone 2011;47(3):519–28.
2 Cheung AM, Adachi JD, Hanley DA, et al. High-resolution peripheral quantitative computed tomography for the assessment of bone strength and structure: A review by the Canadian bone strength working group. Curr Osteoporos Rep 2013;11(2):136–46
3 Boutroy S, Van Rietbergen B, Sornay-Rendu E, Munoz F, Bouxsein ML, Delmas PD. Finite element analysis based on *in vivo* HR-pQCT images of the distal radius is associated with wrist fracture in postmenopausal women. J Bone Miner Res 2008;23(3):392–9.
4 Erlandson MC, Wong AKO, Szabo E, et al. Muscle and Myotendinous Tissue Properties at the Distal Tibia as Assessed by High-Resolution Peripheral Quantitative Computed Tomography. J Clin Densitom 2017;20(2):226–32.
5 Janz KF, Letuchy EM, Burns TL, Francis SL, Levy SM. Muscle Power Predicts Adolescent Bone Strength: Iowa Bone Development Study. Med Sci Sports Exerc 2015;47(10):2201–6.
6 Yingling VR, Webb SL, Inouye C, O J, Sherwood JJ. Muscle Power Predicts Bone Strength in Division II Athletes. J Strength Cond Res 2020;34(6):1657–65.
7 Özçakar L, Çetin A, Ínanici F, Kaymak B, Gürer CK, Kölemen F. Ultrasonographical evaluation of the Achilles' tendon in psoriasis patients. Int J Dermatol 2005;44(11):930–2.
8 Kumar Y, Hayashi D. Role of Imaging in Musculoskeletal Care. Curr Phys Med Rehabil Reports 2016;4(1):28–36.
9 Kruse A, Stafilidis S, Tilp M. Ultrasound and magnetic resonance imaging are not interchangeable to assess the Achilles tendon cross-sectional-area. Eur J Appl Physiol 2017;117(1):73–82.
10 Grimal Q, Laugier P. Quantitative Ultrasound Assessment of Cortical Bone Properties Beyond Bone Mineral Density. IRBM 2019;40(1):16–24.
11 Komar C, Ahmed M, Chen A, et al. Advancing Methods of Assessing Bone Quality to Expand Screening for Osteoporosis. J Am Osteopath Assoc 2019; 119(3):147–54.
12 Chang G, Deniz CM, Honig S, et al. MRI of the hip at 7T: feasibility of bone microarchitecture, high-resolution cartilage, and clinical imaging. J Magn Reson Imaging 2014;39(6):1384–93
13 Liu C, Liu C, Ren X, et al. Quantitative evaluation of subchondral bone microarchitecture in knee osteoarthritis using 3T MRI. BMC Musculoskelet Disord 2017;18(1):496.
14 Wong AK. A comparison of peripheral imaging technologies for bone and muscle quantification: a technical review of image acquisition. J Musculoskelet Neuronal Interact 2016;16(4):265–82.
15 McCloskey EV, Kanis JA, Odén A, et al. Predictive ability of heel quantitative ultrasound for incident fractures: an individual-level meta-analysis. Osteoporos Int. 2015; 26(7):1979-87.
16 Hashemi J, Chandrashekar N, Slauterbeck J. The mechanical properties of the human patellar tendon are correlated to its mass density and are independent of sex. Clin Biomech (Bristol, Avon) 2005;20(6):645–52.
17 Sharma P, Maffulli N. Tendon injury and tendinopathy: healing and repair. J Bone Joint Surg Am 2005; 87(1):187–202.
18 Jones GC, Corps AN, Pennington CJ, et al. Expression profiling of metalloproteinases and tissue inhibitors of metalloproteinases in normal and degenerate human achilles tendon. Arthritis Rheum 2006;54(3):832–42.
19 de Mos M, van El B, DeGroot J, et al. Achilles tendinosis: changes in biochemical composition and collagen turnover rate. Am J Sports Med 2007;35(9):1549–56.
20 Corps AN, Robinson AHN, Movin T, Costa ML, Hazleman BL, Riley GP. Increased expression of aggrecan and

biglycan mRNA in Achilles tendinopathy. Rheumatology (Oxford) 2006;45(3):291–4.
21 Samiric T, Parkinson J, Ilic MZ, Cook J, Feller JA, Handley CJ. Changes in the composition of the extracellular matrix in patellar tendinopathy. Matrix Biol 2009;28(4):230–6.
22 Docking SI, Ooi CC, Connell D. Tendinopathy: Is Imaging Telling Us the Entire Story? J Orthop Sports Phys Ther 2015;45(11):842–52.
23 Klatte-Schulz F, Minkwitz S, Schmock A, et al. Different Achilles Tendon Pathologies Show Distinct Histological and Molecular Characteristics. Int J Mol Sci 2018;19(2).
24 Schepull T, Aspenberg P. Healing of human Achilles tendon ruptures: radiodensity reflects mechanical properties. Knee Surg Sports Traumatol Arthrosc 2015; 23(3):884–9.
25 Fung HJW, Cheung AM, Mathur S, et al. The role of the Achilles tendon in transducing forces from ankle flexor muscles to bone. Appl Physiol Nutr Metab 2018;43(10):S58
26 Pang BSF, Ying M. Sonographic measurement of Achilles tendons in asymptomatic subjects: Variation with age, body height, and dominance of ankle. J Ultrasound Med 2006;25(10):1291–6.
27 Pauchard Y, Liphardt A-M, Macdonald HM, Hanley DA, Boyd SK. Quality control for bone quality parameters affected by subject motion in high-resolution peripheral quantitative computed tomography. Bone 2012;50(6):1304–10.
28 Rosset A, Spadola L, Ratib O. OsiriX: An open-source software for navigating in multidimensional DICOM images. J Digit Imaging 2004;17(3):205–16.
29 Brushøj C, Henriksen BM, Albrecht-Beste E, Hölmich P, Larsen K, Bachmann Nielsen M. Reproducibility of ultrasound and magnetic resonance imaging measurements of tendon size. Acta Radiol 2006; 47(9):954–9.
30 Dudley-Javoroski S, McMullen T, Borgwardt MR, Peranich LM, Shields RK. Reliability and Responsiveness of Musculoskeletal Ultrasound in Subjects with and without Spinal Cord Injury. Ultrasound Med Biol 2010;36(10):1594–607.
31 Santos L, Elliott-Sale KJ, Sale C. Exercise and bone health across the lifespan. Biogerontology 2017;18(6):931–46.
32 Agarwal S, Rosete F, Zhang C, et al. *In vivo* assessment of bone structure and estimated bone strength by first- and second-generation HR-pQCT. Osteoporos Int 2016;27(10):2955–66.
33 Bonaretti S, Vilayphiou N, Chan CM, et al. Operator variability in scan positioning is a major component of HR-pQCT precision error and is reduced by standardized training. Osteoporos Int 2017;28(1):245–57.
34 Boutroy S, Bouxsein ML, Munoz F, Delmas PD. *In vivo* assessment of trabecular bone microarchitecture by high-resolution peripheral quantitative computed tomography. J Clin Endocrinol Metab 2005; 90(12):6508–15.
35 Wong AKO, Beattie KA, Min KKH, et al. A trimodality comparison of volumetric bone imaging technologies. Part I: Short-term precision and validity. J Clin Densitom 2015;18(1):124–35.
36 Engelke K, Adams JE, Armbrecht G, et al. Clinical use of quantitative computed tomography and peripheral quantitative computed tomography in the management of osteoporosis in adults: the 2007 ISCD Official Positions. J Clin Densitom 2008;11(1):123–62.
37 Kawalilak CE, Johnston JD, Olszynski WP, Kontulainen SA. Least significant changes and monitoring time intervals for high-resolution pQCT-derived bone outcomes in postmenopausal women. J Musculoskelet Neuronal Interact 2015;15(2):190–6.
38 Sponbeck JK, Perkins CL, Berg MJ, Rigby JH. Achilles Tendon Cross Sectional Area Changes Over a Division I NCAA Cross Country Season. Int J Exerc Sci 2017;10(8):1226–34.
39 Milgrom Y, Milgrom C, Altaras T, Globus O, Zeltzer E, Finestone AS. Achilles tendons hypertrophy in response to high loading training. Foot Ankle Int 2014; 35(12):1303–8.
40 Romero-Morales C, Martín-Llantino PJ, Calvo-Lobo C, et al. Comparison of the sonographic features of the Achilles Tendon complex in patients with and without achilles tendinopathy: A case-control study. Phys Ther Sport 2019;35:122–6.
41 Magnusson SP, Kjaer M. Region-specific differences in Achilles tendon cross-sectional area in runners and non-runners. Eur J Appl Physiol 2003;90(5–6):549–53.
42 Wearing SC, Grigg NL, Hooper SL, Smeathers JE. Conditioning of the Achilles tendon via ankle exercise improves correlations between sonographic measures of tendon thickness and body anthropometry. J Appl Physiol 2011;110(5):1384–9.
43 Wearing SC, Smeathers JE, Urry S, Hooper SL. The time-course of acute changes in Achilles tendon morphology following exercise. In: Fuss FK, Subic A, Ujihashi S, editors. The Impact of Technology on Sport II. London (UK): Taylor & Francis Group; 2007. p. 65-68.